

The string/gauge theory correspondence in QCD^{*}

Kasper Peeters^{1,a} and Marija Zamaklar^{2,b}

¹ Institute for Theoretical Physics, Utrecht University, P.O. Box 80.195, 3508 TD Utrecht, The Netherlands

² Department of Mathematical Sciences, Durham University, South Road, Durham DH1 3LE, United Kingdom

Abstract. Ideas about a duality between gauge fields and strings have been around for many decades. During the last ten years, these ideas have taken a much more concrete mathematical form. String descriptions of the strongly coupled dynamics of semi-realistic gauge theories, exhibiting confinement and chiral symmetry breaking, are now available. These provide remarkably simple ways to compute properties of the strongly coupled quark-gluon fluid phase, and also shed new light on various phenomenological models of hadron fragmentation. We present a review and highlight some exciting recent developments.

1 Introduction and motivation

Although there are several well-known and clear-cut signs of strings in gauge theories, a concrete realisation of the connection only became available with Maldacena's conjecture of the AdS/CFT correspondence [1]. The crucial new ingredient, namely that strings dual to gauge fields require additional dimensions, had been anticipated by others (see e.g. [2]), but the discovery of D-branes in string theory [3] was necessary to put this idea on a firm footing. Since 1997, the developments have gone essentially two ways. On the one hand, a lot of effort has gone into proving the correspondence as mathematically precise as possible, uncovering intriguing integrable structures along the way. On the other hand, much work has been done on trying to extend the original conjecture from the highly supersymmetric case of [1] to more realistic gauge theories, and QCD in particular.

The generalisation of the AdS/CFT correspondence to more realistic gauge theories, also dubbed AdS/QCD or non-AdS/non-CFT, has been important for two reasons. Firstly, it provides a rigorous basis for many phenomenologically successful string models of strong interactions. It explains how having a four-dimensional gauge theory and at the same time a critical string is compatible, keeping both the good features of phenomenological models and the good features of a tachyon-free quantum conformally invariant string. In this way, one obtains a new way to think about e.g. hadron fragmentation, and also finds new candidates to model the energy distribution of gluon flux tubes as seen on the lattice (see e.g [4]).

Secondly, it provides a way to do dynamical strong coupling calculations at finite temperature. The main driving force here is the discovery of the strongly coupled quark gluon fluid at RHIC (see e.g. [5] for a review). Rather unexpectedly, the quark-gluon fluid has provided string theorists with the long sought-after laboratory in which strongly-coupled gauge theory

^{*} Lectures presented by KP at the 45th Winter School on Theoretical Physics, Feb. 2007, Schladming.

^a e-mail: k.peeters@phys.uu.nl

^b e-mail: marija.zamaklar@durham.ac.uk

dynamics can be explored directly. In return, the AdS/CFT correspondence provides entirely new ways to compute otherwise hard-to-compute properties of the fluid.

By now, the literature on the AdS/CFT correspondence and its generalisation to more realistic gauge theories is huge. Both the attempts to develop a formal proof of the correspondence, as well as the attempts to generalise it to realistic gauge theories, have led to an enormous number of papers. The goal of the present review is to give a concise overview of this vast field, focusing on the applied part of it (the formal side of the field is developing very quickly and there is at present unfortunately no up-to-date review; see e.g. [6] for a somewhat older review text). Starting more or less from scratch, we introduce the basics of the correspondence and then build up to the exciting recent applications to the strongly-coupled quark-gluon fluid.

2 Old and new ideas on strings in gauge theory

2.1 Signs of strings

Long before string theory developed into a theory of quantum gravity, it was known that there are “stringy” features present in gauge theories. One of the mathematically most explicit ways in which strings can be seen to appear is in the limit in which the number of colours N_c is taken large. In this limit, the perturbation series organises itself in an intriguing way [7]. Let us discuss for simplicity the pure-gauge theory, given by the action

$$S = \frac{1}{4g_{\text{YM}}^2} \int d^4x \text{Tr} (F_{\mu\nu} F^{\mu\nu}), \quad F_{\mu\nu} = \partial_\mu A_\nu - \partial_\nu A_\mu + [A_\mu, A_\nu], \quad (A_\mu)_{ij} = A_\mu^a (T^a)_{ij}. \quad (1)$$

Here $(T^a)_{ij}$ are the generators of $\text{SU}(N_c)$. It is convenient to use a graphical notation in which the two indices i, j are each given their own line, the so-called “double-line notation”. The Feynman rules are then as in figure 1.

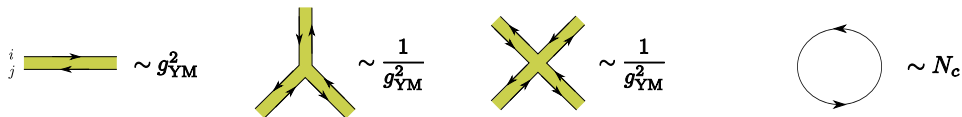


Fig. 1. Feynman rules for $\text{SU}(N)$ gauge theory in the double-line notation. The powers of g_{YM} come from the propagator and vertices, while every closed loop of a black edge yields a power N_c .

Let us look at some simple diagrams and count the powers of g_{YM} and N_c . A number of examples has been drawn in figure 2. They serve to illustrate the following result: by combining the coupling constant and the number of colours into the combination $g_{\text{YM}}^2 N_c$, one can show that the degree of non-planarity of a graph is counted by N_c^{-2} . The planar diagrams all scale like N_c^2 , while non-planar diagrams are suppressed by at least one factor of N_c^{-2} . The combination $g_{\text{YM}}^2 N_c$ is called the “t Hooft coupling” and commonly denoted with λ . By keeping this coupling fixed, we see that the large- N_c expansion is an expansion in the degree of non-planarity, with planar diagrams being the most dominant.

The connection to strings now comes about by trying to figure out how to draw non-planar diagrams as planar ones, making use of surfaces of non-trivial topology. The last diagram of figure 2 is non-planar, but it can be drawn as a planar diagram *on the torus*. This is a general phenomenon: diagrams with a higher degree of non-planarity can be drawn as planar diagrams on surfaces of higher *genus*. In this way, we see that there is a kind of dual relationship between Feynman diagrams of $\text{SU}(N_c)$ gauge theory and two-dimensional surfaces.

These surfaces suggest that there is something stringy about the Feynman diagram expansion. The diagrams can be seen as the duals of Euclidean versions of closed-string world-sheets, with one direction labelling the direction along the string and one direction labelling the evolution in time. Unfortunately, it is very hard to make this relation more precise, or in fact to

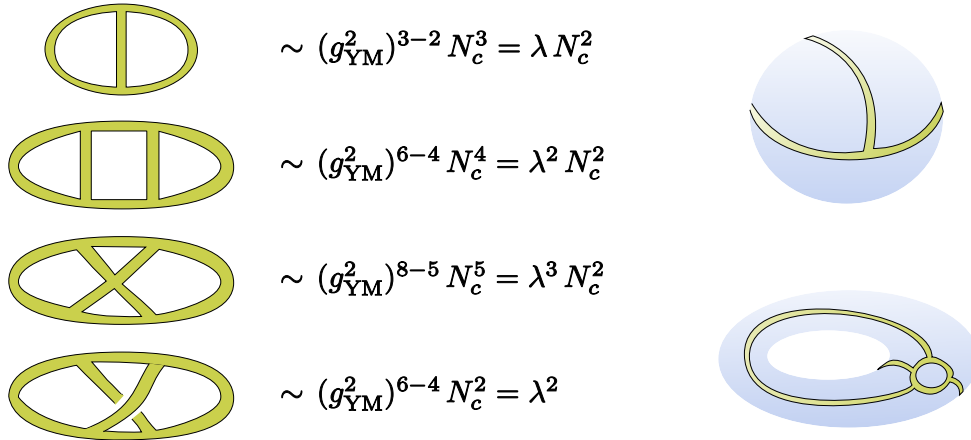


Fig. 2. Counting powers of g_{YM} and N_c . By combining the coupling constant and the number of colours into the so-called 't Hooft coupling $\lambda = g_{\text{YM}}^2 N_c$, one sees that N_c^{-2} counts the degree of non-planarity (left). Planar diagrams can be drawn planar on a sphere, while non-planar diagrams require higher-genus surfaces in order to be drawn as planar graphs (right).

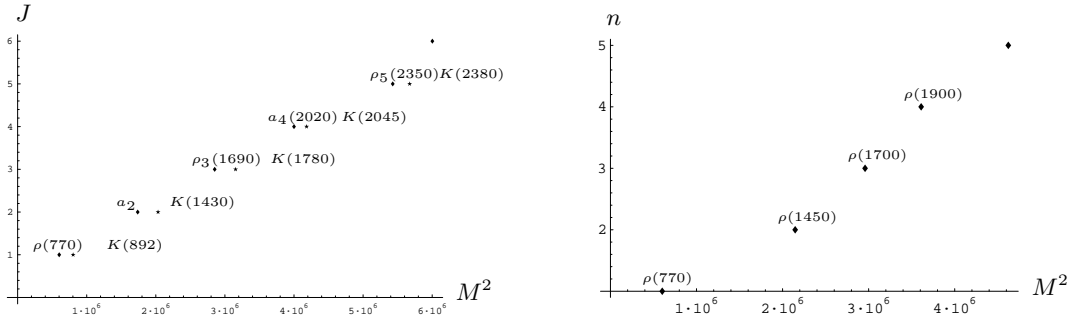


Fig. 3. Regge trajectories of mesons relate the spin J to the mass-squared M^2 (left) or the excitation level n to the mass-squared (right) [10].

use it to compute Feynman diagrams (a recent fresh approach to this program can be found in [8]). One of the main puzzles is that, even though we have identified the meaning of N_c , we still do not know what is the meaning of the 't Hooft coupling λ in terms of the string theory.

String features of gauge theory are, however, not only visible in perturbation theory around weak coupling. They are also manifest in the *strong coupling* regime, where there are obvious signs of the presence of string-like forces. This is in particular clear by looking at the spectrum of mesons or baryons. These spectra display, to good approximation, a linear relation between the spin J and the mass-squared M^2 ,

$$J = \alpha + \alpha' M^2, \quad (2)$$

with different trajectories distinguished by different intercepts α , yet having an almost identical slope α' . A similar linear Regge relation can be seen by keeping the spin fixed but looking instead at the excitation level n (see figure 3). These linear relations are easily obtained from a string-like model of mesons, in which mesons are seen as massive quarks or di-quarks connected by a relativistic string (see e.g. [9] for a recent review). While suggestive, this again leaves us with the problem of understanding the meaning of the 't Hooft coupling.

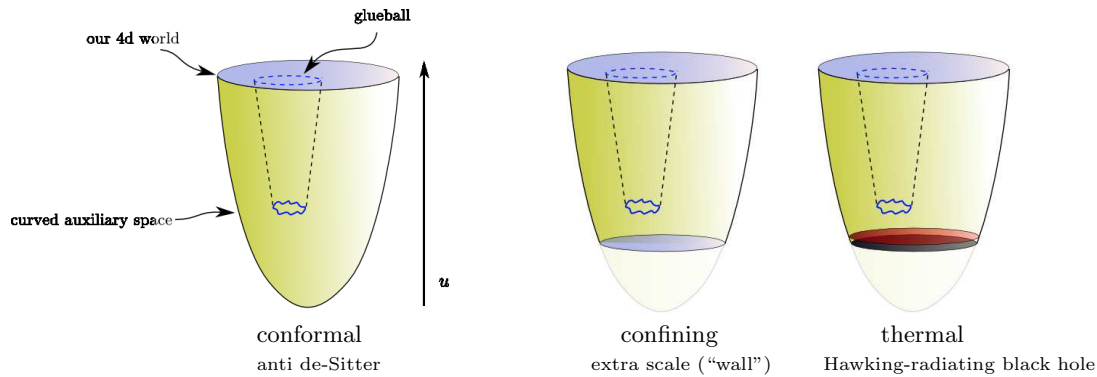


Fig. 4. Symbolic depiction of the basic idea of the AdS/CFT correspondence: the string theory dual to gauge theory is higher-dimensional. The string lives in a curved space-time, and there is a specific map which relates the physics of the string to the physics in our four-dimensional world. More recent extensions of this conjecture have produced string geometries dual to confining and thermal theories (right).

2.2 The AdS/CFT correspondence

The AdS/CFT correspondence, first conjectured by Maldacena [1] based on earlier work by Polyakov [2], gives a concrete handle on the meaning of the 't Hooft coupling λ , as well as a concrete answer to the question “where is the QCD string?”. The key ingredient is that the strings of the theory dual to gauge theory do not reside in our four-dimensional world, but are instead contained in an auxiliary, higher-dimensional curved space-time. There exists a specific and well-defined map between the calculations which one can do with the strings in this higher dimensional space and the calculations one can do in the four-dimensional gauge theory; we will return to this map shortly.

In the original and best-understood form of this conjecture, the curved string space-time is five-dimensional Anti-de-Sitter space times a five-sphere, $\text{AdS}_5 \times S^5$, and the dual gauge theory lives on its boundary, $\mathbb{R} \times S^3$. Importantly, it gives a precise relation between the 't Hooft coupling and parameters on the string theory side,

$$\lambda = \frac{R^4}{(l_{\text{string}})^4}, \quad (3)$$

where R is the radius of curvature of the AdS_5 space-time, and l_{string} is the string length (we will also use $\alpha' = (l_{\text{string}})^2$). When the curvature radius is very large compared to the typical size of the string, $R \gg l_{\text{string}}$, only the massless states in the spectrum of the string survive, and one ends up with a *gauge/gravity* correspondence. In this regime, where string theory is best under control, the gauge theory is strongly coupled. By now, it is also known which qualitative features of the string geometry have to be modified in order to generalise the correspondence to confining and thermal gauge theories (see figure 4). In all of these cases, we have a relation similar to (3), stating that weakly coupled strings are dual to a strongly coupled gauge theory.

How does one arrive at such an idea? It arose by carefully analysing the dynamics of D-branes in string theory. D-branes are very massive objects in the spectrum of relativistic strings [3]. To first approximation, one can think of them as fixed hypersurfaces in space-time, which yield Dirichlet boundary conditions for light strings (see figure 5). Depending on which string theory one is working with, they come in various dimensionalities. In the type-IIB string theory, one finds in particular 3+1 dimensional D3-branes. The key idea is now to look at a stack of N_c of these. Each of the N_c D3-branes couples to the gravitational degrees of freedom with a strength g_s , so in total the strength of the gravitational distortion depends on $g_s N_c$. There are now two regimes in which we can consider the system.

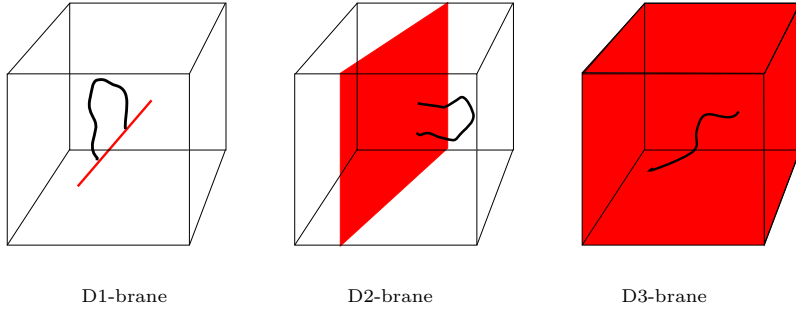


Fig. 5. The theory of open strings contains various heavy objects in its spectrum, which can be interpreted as boundary conditions on the endpoints of the light open strings.

When $g_s N_c \ll 1$, space-time is nearly flat. The fluctuations of the D-brane are described by open strings. There are also closed strings, but they decouple from the open strings because the string coupling is weak. If we focus on low-energy excitations, these closed string degrees of freedom describe a decoupled linearised gravity theory. The open string low-energy degrees of freedom are described by the open string effective action, which is a super-Yang-Mills theory on the D-brane.

When $g_s N_c \gg 1$, back-reaction of the branes on the background becomes important, and space-time is curved. This curvature is described in terms of the effective action for closed strings, i.e. the supergravity theory in the full space-time (the “bulk”). If we look at low-energy excitations as seen from an observer at infinity, these are essentially the excitations close to the horizon, as those are strongly red-shifted. These excitations cannot easily escape to the asymptotic region. Moreover, low-energy excitations from the asymptotic regime find it hard to probe the near-horizon regime, because their wavelength is so large. Therefore, we again find two decoupled theories, one describing linearised gravity in the asymptotic region, and one describing gravity in the near-horizon region.

Thus, the asymptotic region is, both in the $g_s N_c \ll 1$ and in the $g_s N_c \gg 1$ regime, described by decoupled linearised gravity. Since it is decoupled, we are left with the effective action for *open* strings in flat space-time when $g_s N_c \ll 1$, and the effective action for *closed* strings in the near-horizon region when $g_s N_c \gg 1$. The statement of the string/gauge theory correspondence is now that the gauge theory describing the open strings on the D3-brane and the supergravity theory describing the closed strings in the near-horizon regime of the curved D3-brane supergravity solution are two *different* descriptions of the *same* physical system.

More precisely, the open string degrees of freedom are described by a four-dimensional Dirac-Born-Infeld action for the gauge fields (see e.g. [11]), which at lowest order in derivatives reduces to $N = 4$ super-Yang-Mills,

$$S = \frac{1}{g_{\text{YM}}^2} \int d^4x \text{Tr} \left(\frac{1}{4} F_{\mu\nu} F^{\mu\nu} + \frac{1}{2} (D_\mu \phi_{ij})^2 + \frac{1}{2} \bar{\chi}_i \not{D} \chi_i - \frac{1}{2} \bar{\chi}_i [\phi_{ij}, \chi_j] - \frac{1}{4} [\phi_{ij}, \phi_{kl}] [\phi_{ij}, \phi_{kl}] \right) \quad (4)$$

with 6 adjoint scalars $\phi^{(ij)}$, a gauge field A_μ and 4 chiral adjoint fermions χ_i . The closed strings are, for large values of λ , described by supergravity excitations around the near-horizon geometry of the extremal D3-brane. The metric of the D3-brane is [12],

$$ds^2 = \left(1 + \frac{R^4}{u^4} \right)^{-1/2} (-dt^2 + dx_1^2 + dx_2^2 + dx_3^2) + \left(1 + \frac{R^4}{u^4} \right)^{1/2} (du^2 + u^2 d\Omega_5^2). \quad (5)$$

This has a horizon at $u = 0$ (these are isotropic coordinates), as $g_{tt} \rightarrow 0$ there. There is also a five-form field, whose charge is fixed by the supergravity equations of motion to

$$\int_{S^5} F_5 = N_c, \quad \text{and} \quad 4\pi g_s N_c l_s^4 = R^4, \quad (6)$$

where g_s is the string coupling constant. The conjecture says that we should go close to the horizon of the D3-brane, where we end up with the metric

$$ds^2 = \frac{u^2}{R^2} (-dt^2 + dx_1^2 + dx_2^2 + dx_3^2) + \frac{R^2}{u^2} du^2 + R^2 d\Omega_5^2. \quad (7)$$

This is the $\text{AdS}_5 \times S^5$ metric on which the string theory dual to the gauge theory lives (one often also uses a coordinate $z = 1/u$ which makes the conformal equivalence of AdS_5 to flat space come out more clearly). More formally, the correspondence thus states that type-IIB string theory on the background (7) is equivalent to the gauge theory described by (5) on the $\mathbb{R} \times S^3$ boundary.¹

2.3 The holographic dictionary

Let us now discuss in some detail how computations done on the string theory side can be related to those which one would like to do on the gauge theory side. The relation between correlation functions on the two sides which we will discuss below was first proposed in [13, 14]. The connection is made at the level of the generating functional for correlation functions. In a nutshell, the connection is written as

$$\begin{aligned} Z_{\text{string}} &= \exp \left[-S_{\text{sugra}} \left(\phi(t, \mathbf{x}; u = \infty) = u^{\Delta-4} \phi_0(t, \mathbf{x}) \right) \right] + \dots \\ &= \left\langle T \exp \int d^4x \phi_0(t, \mathbf{x}) \mathcal{O}(t, \mathbf{x}) \right\rangle_{\text{field theory}}. \end{aligned} \quad (8)$$

Let us explain this in some detail. The field $\phi(t, \mathbf{x}; u)$ is a field on the $\text{AdS}_5 \times S^5$ geometry, for instance a graviton fluctuation. It is a function of all five coordinates, in particular the radial direction u of the metric (7). Near the boundary, the fluctuations scale with u according to their conformal dimension Δ . The first line of the expression above instructs us to evaluate the string partition function, which to first order is given by the exponent of the supergravity action, given a certain boundary behaviour of the field ϕ . The correspondence now states that the result is the same as computing the field theory expectation value of the exponent of a specific operator \mathcal{O} , coupled to $\phi_0(t, \mathbf{x})$, now interpreted as a source.

Correlation functions on the gauge theory side now follow simply by computing repeated derivatives with respect to the source,

$$\frac{\delta^n Z_{\text{string}}}{\delta \phi_0(t_1, \mathbf{x}_1) \cdots \delta \phi_0(t_n, \mathbf{x}_n)} = \left\langle T \mathcal{O}(t_1, \mathbf{x}_1) \cdots \mathcal{O}(t_n, \mathbf{x}_n) \right\rangle_{\text{field theory}}. \quad (9)$$

It is illustrative to discuss this method of computing correlators for at least one simple example. So let us discuss the canonical one, namely the two-point function of a massive scalar field (see e.g. [15, 16, 17]). The action for a massive scalar field on AdS_5 is given by (using $z = 1/u$)

$$S = \frac{1}{g_s^2} \int_0^\infty dz d^4x \frac{1}{z^3} \left[(\partial_z \phi)^2 + (\partial_\mu \phi)^2 + \frac{m^2 R^2}{z^2} \phi^2 \right]. \quad (10)$$

If we want correlation functions in the boundary theory in momentum space, we should make an expansion of the field $\phi(x^\mu; z)$ in terms of z -dependent modes $f_k(z)$ and boundary fields $\phi_0(k_\mu)$,

$$\phi(x^\mu; z) = \int \frac{d^4k}{(2\pi)^4} e^{ik \cdot x} f_k(z) \phi_0(k_\mu). \quad (11)$$

¹ Strictly speaking, the boundary of (7) is $\mathbb{R} \times \mathbb{R}^3$. Both $\mathbb{R} \times S^3$ and $\mathbb{R} \times \mathbb{R}^3$ can be viewed as the boundary of AdS_5 as they are related by a conformal transformation if the point at infinity in \mathbb{R}^3 is included.

This yields the action

$$S = \frac{1}{g_s^2} \int_0^\infty dz \int \frac{d^4 k d^4 k'}{(2\pi)^8} \frac{1}{z^3} \left[\partial_z f_k \partial_z f_{k'} + k^2 f_k f_{k'} + \frac{m^2 R^2}{z^2} f_k f_{k'} \right] \phi_0(k_\mu) \phi_0(k'_\mu) \delta^{(4)}(k+k'). \quad (12)$$

By partially integrating the first term in the action with respect to z , we find the equation of motion for f_k plus a boundary term,

$$S_{\text{on shell}} = \frac{1}{g_s^2} \int \frac{d^4 k d^4 k'}{(2\pi)^8} \delta^{(4)}(k+k') \phi_0(k_\mu) \phi_0(k'_\mu) \left. \frac{f_{k'} \partial_z f_k}{z^3} \right|_\epsilon^\infty, \quad (13)$$

where we have regulated the boundary using a small parameter ϵ . By taking two variational derivatives with respect to the “source” $\phi_0(k)$, as in (9), we thus immediately read off an expression for the two-point function in $N = 4$ super Yang-Mills.

In order to compute it, we need to solve the equation of motion for the z -dependent part of the solution. It is given by

$$f_k'' - \frac{3}{z} f_k' - \left(k^2 + \frac{m^2 R^2}{z^2} \right) f_k = 0. \quad (14)$$

This equation has the general solution

$$f_k = C_1 z^2 I_{\Delta-2}(kz) + C_2 z^2 K_{\Delta-2}(kz), \quad \Delta = 2 + \sqrt{4 + m^2 R^2}, \quad (15)$$

where $I_{\Delta-2}$ and $K_{\Delta-2}$ are modified Bessel functions of the first and second kind. Imposing regularity in the interior at $z = \infty$ forces us to set $C_1 = 0$; normalising the remaining solution to one at $z = \epsilon$ (i.e. near the boundary), we end up with

$$f_k(z) = \frac{z^2 K_{\Delta-2}(kz)}{\epsilon^2 K_{\Delta-2}(k\epsilon)}. \quad (16)$$

Inserting this in (13), we find a contribution from the $z = \epsilon$ boundary which is given by

$$\langle \mathcal{O}(k) \mathcal{O}(k') \rangle = \epsilon^{2(\Delta-2)} \delta^{(4)}(k+k') k^{2(\Delta-2)} 2^{1-2(\Delta-2)} \frac{\Gamma(3-\Delta)}{\Gamma(\Delta-1)} (\Delta-2) + \dots, \quad (17)$$

plus contact terms. The details are not very important at this stage (and there are several subtleties in identifying which are the gauge theory operators \mathcal{O} and how to normalise them properly, which we have not discussed). What is important is the general logic. A priori, there are two independent solutions for f_k near the boundary. Imposing regularity of the supergravity solutions in the interior removes one of the coefficients and leaves only an overall normalisation. The boundary term in the action then leads to the correlator of the dual gauge theory operators. This logic holds also for more complicated string/gauge theory duals.

The spectrum of the bulk modes satisfying equations such as (14) is in one-to-one relation with the spectrum of gauge invariant operators in the boundary theory. This connection is at the basis of computations of gauge theory spectra (for instance of glueballs [18, 19]) by solving supergravity spectral problems. We will see this connection for mesons in more detail in later sections.

Apart from computing correlators or the spectrum of physical states, one is often also interested in vacuum expectation values of certain operators. The value of a bulk field at the boundary is related, by the holographic dictionary, to a chemical potential. By varying this leading component μ of the boundary field $\phi_0(t, \mathbf{x}; z)$ (the “non-normalisable mode”), we can compute the expectation value of the dual operator in a particular state. The logic is similar to the one above for correlators. By varying the boundary field, one ends up with an equation of motion plus a boundary term,

$$\delta S = \text{EOM}_{\text{bulk}} + \left(\frac{\partial S}{\partial \phi} \frac{\delta \phi}{\delta \mu} \delta \mu \right)_{\text{boundary}} = \text{EOM}_{\text{bulk}} + \delta \mu \langle O_\mu \rangle. \quad (18)$$

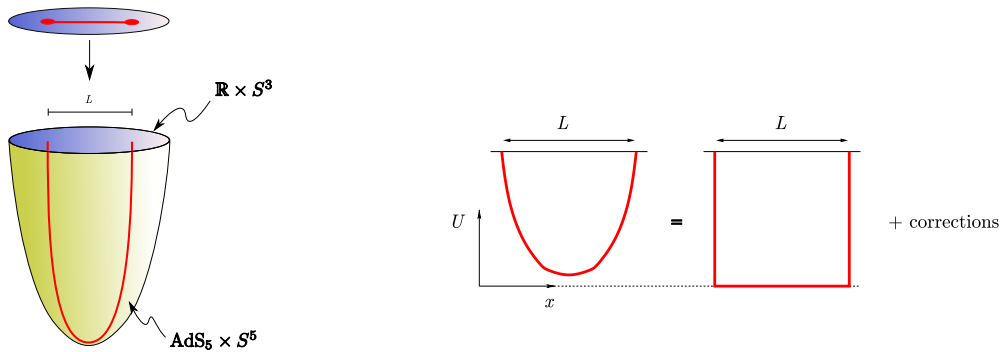


Fig. 6. In order to get a confining quark/anti-quark potential, the Wilson loop in the gauge theory should exhibit an area law. This requires that the string stretching in the higher-dimensional space has a long horizontal segment. Conformal invariance prevents this (left), but there are other metrics which do allow for such a configuration (right).

If one writes this in a series expansion near the boundary, one finds that whereas μ is the coefficient of the leading term, the expectation value $\langle \mathcal{O} \rangle$ is related to the subleading or “normalisable” coefficient of the bulk field.

One final comment concerns the meaning of the radial direction. The cut-off ϵ is an ultraviolet cut-off in the dual gauge theory. The radial direction u is therefore related to the energy scale in the dual gauge theory. Strongly coupled infrared physics in the gauge theory is related to string phenomena which happen deep inside the bulk of the supergravity solution.

3 String duals with confinement and chiral symmetry breaking

3.1 From Coulomb potentials to confining potentials

Having access to a string dual of $N = 4$ super-Yang-Mills, the question of course arises as to whether it is possible to use the same idea to construct string duals of more realistic gauge theories. In particular, it would be interesting to find a string dual to a gauge theory which exhibits confinement.

Recall that a signal for confinement can be found in the behaviour of Wilson loop. For $N = 4$ super-Yang-Mills, the string configuration dual to a Wilson loop is a string world-sheet ending with its boundary on the Wilson loop; a slice at constant time is drawn in figure 6. The energy of this string configuration can be computed, and turns out to scale as [20]

$$E \sim L^{-1}, \quad (19)$$

i.e. it exhibits a Coulomb potential. In order to obtain a string dual to a confining theory, we somehow need to construct a curved string background which is such that the U-shaped string has a long horizontal segment with an effective non-zero string tension. For the $\text{AdS}_5 \times S^5$ geometry, this long horizontal segment is missing, and we therefore do not obtain the linear scaling of energy with distance.

Following [21], we can investigate the generic behaviour of E as a function of the endpoint separation L as follows. Consider a generic background metric, with a time-like direction t , space-like directions x^i and a radial direction u , together with a number of transverse coordinates x_T which do not play a role. The line element is given by

$$ds^2 = -g_{tt}(u) dt^2 + g_{xx}(u)(dx^2 + dy^2 + dz^2) + g_{uu} du^2 + g_{TT}(u) dx_T^2. \quad (20)$$

The string will be a U-shape extending in the energy direction u and the space direction x , as in figure 6. In the gauge $\tau = t$, $\sigma = x$, the action for this string is

$$S_{\text{Wilson}} = \int d\tau d\sigma \mathcal{L} = T \int dx \sqrt{g_{tt}(u)g_{xx}(u) + g_{tt}(u)g_{uu}(u) \left(\frac{\partial u}{\partial x}\right)^2}. \quad (21)$$

Making use of the fact that this expression does not depend explicitly on x , one can compute the conserved ‘‘Hamiltonian’’ associated to translations in x , and from there compute

$$\frac{\partial u}{\partial x} = \pm \sqrt{\frac{g_{tt}(u)}{g_{uu}(u)}} \sqrt{\frac{g_{tt}(u)g_{xx}(u) - g_{tt}(u_0)g_{xx}(u_0)}{g_{tt}(u_0)g_{xx}(u_0)}}} \rightarrow \mathcal{L}_{\text{on shell}} = \frac{g_{tt}(u)g_{xx}(u)}{\sqrt{g_{tt}(u_0)g_{xx}(u_0)}}. \quad (22)$$

Here u_0 is the lowest point reached by the string, where it is assumed that $g_{tt}g_{xx}$ has a minimum or $g_{tt}g_{uu}$ diverges. This is all that is needed in order to compute the four-dimensional length L and the energy E ,

$$L = \int dx = \int du \frac{\partial x}{\partial u}, \quad E = \int dx \mathcal{L} = \int du \frac{\partial x}{\partial u} \mathcal{L}. \quad (23)$$

The energy contains a term linear in the length L plus a correction term,

$$E = \sqrt{g_{tt}(u_0)g_{xx}(u_0)} L + K(u_0), \quad (24)$$

where $K(u_0)$ can be found in [21]. The idea now is that the lowest part of the string is very close to the bottom of the geometry, i.e. $u_0 \approx 0$, so that $\sqrt{g_{tt}(u_0)g_{xx}(u_0)} \approx \sqrt{g_{tt}(0)g_{xx}(0)}$. This factor then acts as an effective string tension T_{eff} . In [21] it was shown that if the tension is non-zero, and monotonic in u with a minimum at $u = 0$, and if all integrals converge, then $K(u_0)$ is a correction which scales as a negative power of L or is exponentially small in L .

One way to achieve a non-zero tension and a linear potential therefore is to ‘‘cut off’’ the AdS factor at some finite radius $u = u_{\text{wall}}$. This is the so-called ‘‘hard wall approximation’’ (see e.g. [22, 23, 24]). It has the advantage that one can compute with the relatively simple AdS₅ metric, in which many results can be obtained analytically (see [25, 26] for the state of the art of these and related models). However, such an artificial cut-off of the AdS radius does not satisfy the supergravity equations of motion, and one runs the risk that the dynamics of the gauge theory is not correctly encoded. A more natural way to achieve a cut-off is to make use of a supergravity solution which contains an extra dimension which shrinks to zero size at a finite value for the radial distance u . This is similar to the way in which one can make the boundary of a half-line smooth by turning it into a thin cigar. Such a situation occurs in many other D-brane metrics. An example is

$$ds^2 = \left(\frac{u}{R_{\text{D4}}}\right)^{\frac{3}{2}} [\eta_{\mu\nu} dX^\mu dX^\nu + f(u) d\theta^2] + \left(\frac{R_{\text{D4}}}{u}\right)^{\frac{3}{2}} \left[\frac{du^2}{f(u)} + u^2 d\Omega_4 \right], \quad f(u) = 1 - \left(\frac{u_\Lambda}{u}\right)^3. \quad (25)$$

This metric is obtained by doubly Wick rotating the the near-horizon metric of a near-extremal D4-brane [27] (we use here the coordinates of e.g. [28, 29]). The geometry of this space-time is depicted in figure 7. The main feature is that the θ circle shrinks to zero size at $u = u_\Lambda$, leading to a cigar-like subspace. Near the tip of this cigar, the circle is small, and the theory is effectively four-dimensional. The model breaks conformal invariance and has a single mass scale.²

The minimum of $g_{tt}g_{xx}$ now occurs at the tip of the cigar, where the value is still non-zero. This leads to an effective string tension given by

$$T_{\text{eff}} = \frac{1}{2\pi\alpha'} \sqrt{-g_{tt}g_{xx}} \Big|_{u=u_\Lambda} = \frac{1}{2\pi\alpha'} \left(\frac{u_\Lambda}{R_{\text{D4}}}\right)^{3/2}. \quad (26)$$

In order to avoid a conical singularity in the $u - \tau$ plane, the angular coordinate θ has to be identified with period

$$\theta \simeq \theta + L_\Lambda, \quad \text{with} \quad L_\Lambda = \frac{4}{3}\pi \sqrt{\frac{R_{\text{D4}}^3}{u_\Lambda}}. \quad (27)$$

² There are various other approaches to the construction of confining backgrounds [30, 31, 32], which we will not discuss here; for a review see [33].

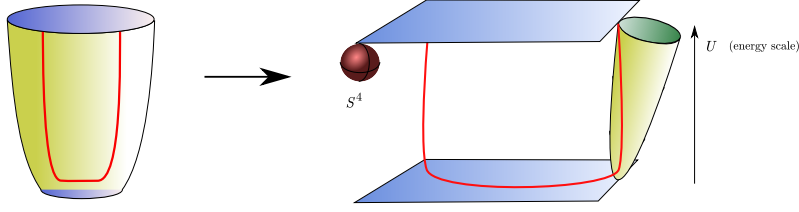


Fig. 7. The geometry of the D4-brane background: instead of introducing a hard cut-off in AdS_5 (left), the main new ingredient is a circle spanned by the θ coordinate which shrinks to zero size at some finite value of the radial direction u , making the geometry everywhere smooth (right).

Recall that the $\text{AdS}_5 \times S^5$ case, an analysis of the supergravity solution led to the relation $g_s N_c = R^4/l_s^4$. A similar analysis now leads to $g_s N_c = R_{\text{D4}}^3/l_s^3$. The five-dimensional 't Hooft coupling (dimensionful) is given by $\lambda_5 = g_s N_c l_s$ and the four-dimensional one is $\lambda_4 = \lambda_5/L_A$, so that

$$\lambda_4 = \frac{R_{\text{D4}}^3}{l_s^2 L_A}, \quad (28)$$

to be compared with (3). Recall also that all physical quantities in the $\text{AdS}_5 \times S^5$ case are expressed in terms of the dimensionless ratio R^4/l_s^4 ; similarly, l_s disappears from physical quantities in the model discussed here. Notice the appearance of the extra mass scale, $M_A = 2\pi/L_A$.

3.2 Adding flavour degrees of freedom

Having obtained a confining potential, the second thing we need to do is to introduce matter in the fundamental representation of the gauge group. The way to achieve this was first proposed by [34]³, and consists of adding, on top of the supergravity background, a number of extra branes. These extra branes are called “flavour branes”. First of all, they introduce new degrees of freedom corresponding to strings stretching between the original branes and the new flavour branes. These correspond to quarks in the fundamental representation (and the number of branes thus corresponds to the number of flavours in the gauge theory). Secondly, there are new degrees of freedom corresponding to open strings ending with both ends on the flavour branes. These, as we will see, correspond to bound states of quarks and anti-quarks, i.e. mesonic degrees of freedom. The string/gauge correspondence then makes a prediction for the masses and couplings of these mesons.

The largest dimension which a flavour brane can have while still being non-trivial is $8 + 1$, a so-called D8-brane. This leaves one function to specify the embedding of the brane in the background (25). This embedding will be discussed below; it is illustrated in figure 8. It turns out that the fluctuation spectrum of this model leads to chiral fermions [36]. However, there are of course many other setups which one can study. The original analysis of [34] employed a D7-brane added to the $\text{AdS}_5 \times S^5$ background, i.e. a D3-D7 system. This is still the basis of much qualitative work, because the simplicity of the metric makes it possible to obtain many results analytically (see e.g. [37]). An alternative setup using the D4-brane background is to introduce a D6-brane [38]. The latter model exhibits an interesting phase diagram, but unfortunately does not contain chiral fermions, so we will refrain from discussing it here.

Let us now turn to a more quantitative analysis. The shape of the D8 flavour brane can be found by simply solving the equation of motion. The action for the D8-brane in the background (25) is given by

$$S_{\text{D8}} \propto \int d^4x d\theta u^4 \sqrt{f(u) + \left(\frac{R_{\text{D4}}}{u}\right)^3 \frac{(u')^2}{f(u)}}, \quad (29)$$

³ Flavour branes were first introduced into confining backgrounds in [35].

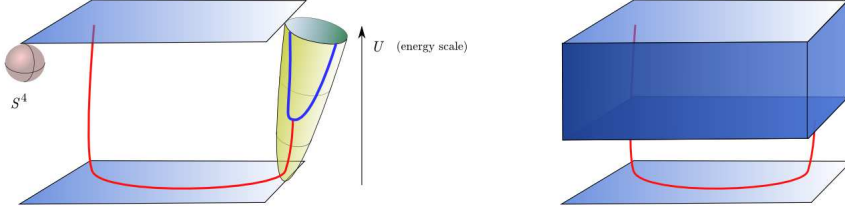


Fig. 8. A D8 flavour brane in the Sakai-Sugimoto model fills all of space except for one direction, thus leading to a curve $u = u(\theta)$. The picture on the right shows the same configuration with all directions except x^1, x^2 and u suppressed. In this picture, the situation looks like a brane “ending in thin air”. The long, almost rectangular curve $u(x^1)$ depicts a $J \gg 1$ meson or static Wilson loop.

where $u' = du/d\theta$. Because the action does not depend explicitly on the θ coordinate there is a conserved charge associated to translations in θ . This charge can be found by computing the associated “Hamiltonian”, which reads

$$\mathcal{H} = \frac{d\mathcal{L}}{d\theta} u' - \mathcal{L} = \frac{u^4 f(u)}{\sqrt{f(u) + \left(\frac{R_{D4}}{u}\right)^3 \frac{(u')^2}{f(u)}}} = u^8 f(u) \mathcal{L}^{-1}. \quad (30)$$

From $d\mathcal{H}/d\theta = 0$ we then find for the embedding

$$\theta = u_0^4 \sqrt{f(u_0)} \int_{u_0}^u \frac{du}{\left(\frac{u}{R_{D4}}\right)^{3/2} f(u) \sqrt{u^8 f(u) - u_0^8 f(u_0)}}. \quad (31)$$

Here u_0 is a free integration constant, denoting the lowest point on the u axis which is reached by the D8-brane. The shape $\theta(u)$ is depicted in figure 8. Even though this shape is thus only known implicitly and can at best be evaluated numerically, the result (31) is sufficient to study the meson spectrum in this model. The u_0 parameter is related to the constituent quark mass, as we will discuss in section 3.3.

The model is invariant under gauge transformations of the gauge field living on the world-volume of the D8-branes. Large gauge transformations, which asymptote to a constant independent of x^μ as the boundaries at $u \rightarrow \infty$ are approached, correspond to global symmetries of the boundary theory. Because there are two boundaries, there is a priori a $U(N_f) \times U(N_f)$ global symmetry, which is indeed the chiral symmetry of the fermions. However, the gauge transformations on these two sides of the brane have to connect smoothly at the bottom, which reduces the freedom to only $U(N_f)$. Hence, the connectedness of the two halves of the D8-brane stack is the dual of chiral symmetry breaking.

In all models with flavour branes, there are two regimes in which we can study mesons. One regime is that of *small spin* mesons, for spins $J \leq 1$. These correspond to small fluctuations of the flavour brane. The masses of these states turn out to scale just like the glueball masses (which we have not discussed explicitly, but arise from the fluctuation spectrum of bulk modes as we mentioned briefly in section 2.3). Explicitly, $M_{\text{small spin}} \sim M_A$; we will discuss these mesons shortly. The other regime is that of *large spin* mesons, for $J \gg 1$. These mesons are described by long macroscopic strings, which have their endpoints attached to the flavour brane. Their masses are set by the effective string tension at $u = u_A$, which leads to $M_{\text{large spin}} \sim \sqrt{\lambda} M_A$. In the supergravity regime, these states are thus anomalously heavy compared to the small-spin ones. We will discuss the large spin mesons in section 3.3.

The small-spin meson spectrum contains scalar mesons, arising from the fluctuation of the embedding coordinates of the D8-brane, as well as vector mesons, arising from the vector fields on the brane. We can construct an effective action for them by following the logic which we discussed for the bulk modes in section 2.3. Let us focus on the vector mesons. We start from

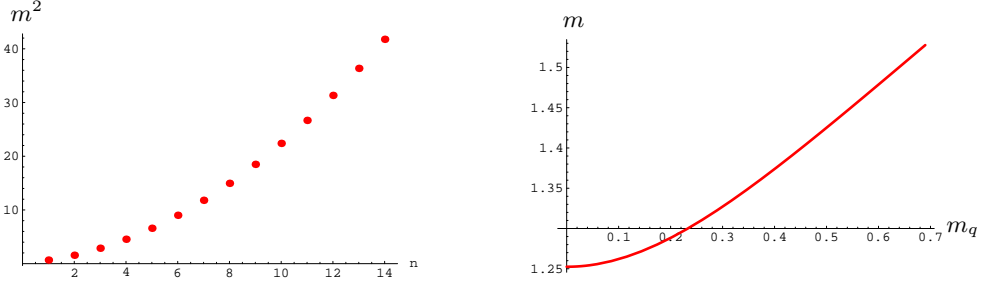


Fig. 9. The first few states of the vector meson mass spectrum of the Sakai-Sugimoto model (left) and the behaviour of the ‘ a_1 ’ meson mass as a function of the constituent quark mass (right).

the action of the D8-brane, which is

$$S = V_{S^4} \int d^5x e^{-\phi} \sqrt{-\det(g_{\mu\nu} + 2\pi\alpha' F_{\mu\nu})} = \tilde{V}_{S^4} \int d^5x \sqrt{-g} F_{\mu\nu} F_{\rho\lambda} g^{\mu\rho} g^{\nu\lambda} + \dots \quad (32)$$

(There is also a Wess-Zumino term, which however plays no role for the determination of the meson spectrum here). Using the background metric (25) and the embedding equation (31), we get more explicitly

$$S = \tilde{V}_{S^4} \int d^4x du \left[u^{-1/2} \gamma^{1/2} F_{\mu\nu} F_{\mu\nu} + u^{5/2} \gamma^{-1/2} F_{\mu u} F_{\mu u} \right], \quad (33)$$

where all indices are now contracted with the flat metric and $\gamma = u^8 / (u^8 f(u) - u_0^8 f(u_0))$.

We now decompose the fields in terms of a four-dimensional factor and a u -dependent one, as in

$$\begin{aligned} F_{\mu\nu} &= \sum_n G_{\mu\nu}^{(n)}(x) \psi_{(n)}(u), \\ F_{u\mu} &= \sum_n B_\mu^{(n)}(x) \partial_u \psi_{(n)}(u), \end{aligned} \quad \text{where} \quad B_\mu^{(m)}(x) = \int \frac{d^4k}{(2\pi)^4} e^{ik_\mu x^\mu} B_\mu^{(m)}(k). \quad (34)$$

Here $G_{\mu\nu}^{(n)}$ is the field strength for $B_\mu^{(n)}$. Inserting these expansions, the polarisation vectors can be factored out, and we end up with the following equation of motion for the modes $\psi_{(n)}(u)$,

$$\int d^4x B_\mu^{(m)} B_\mu^{(n)} \left[u^{-1/2} \gamma^{1/2} (\omega^2 - \mathbf{k}^2) \psi_{(n)} - \partial_u \left(u^{5/2} \gamma^{-1/2} \partial_u \psi_{(n)} \right) \right] = 0. \quad (35)$$

If the equation of motion inside the brackets is satisfied for a particular $\omega^2 - \mathbf{k}^2$, and the solution is inserted back into the action (33), we end up with an action for massive vector fields $B_\mu^{(n)}$.

Thus, in order to find the meson spectrum, we have to solve the Sturm-Liouville problem of (35). The solutions $\psi_{(n)}$ have to be finite on the entire D8-brane, i.e. on both ends of the U-shaped embedding. In order to have access to these two sides, one introduces a new coordinate z by

$$u = (u_0^3 + u_0 z^2)^{1/3}. \quad (36)$$

In this coordinate system, the two asymptotic ends of the D8-brane are at $z \rightarrow +\infty$ and $z \rightarrow -\infty$ respectively. Solving the eigenvalue problem (35) is possible for generic embedding, but the equations are simplest in the case that the D8-brane goes through the tip of the cigar, i.e. when $u_0 = u_\Lambda$ (which makes $\gamma = f^{-1}$).

Let us first look at the massless sector. We will see that this contains pions described by a chiral Lagrangian. In the z coordinate, there are two zero-mass modes (cf. (35)), being combinations of a normalisable and a non-normalisable one near the two boundaries,

$$\psi_+ = \frac{1}{2}(1 \pm \psi_0), \quad \psi_0 = \frac{2}{\pi} \arctan z. \quad (37)$$

For the expansion we use (in the $A_z = 0$ gauge)

$$A_\mu = i\xi_+ \partial_\mu \xi_+^{-1}(x) \psi_+(z) + i\xi_- \partial_\mu \xi_-^{-1}(x) \psi_-(z), \quad (38)$$

where we will leave ξ_+ and ξ_- arbitrary for the time being; the presence of two modes reflects that there is still a residual gauge invariance present. For the holographic derivation of the chiral Lagrangian for pions, we focus on the $F_{\mu z}^2$ term, do one partial integration in the z direction and thus write the action as

$$\begin{aligned} S &= \text{EOM} + \int d^4x \text{Tr} (A_\mu F_{\mu z}) (1+z^2) \Big|_{z=-\infty}^{\infty} \\ &= \text{EOM} + \int d^4x \text{Tr} \left[\xi_+ \partial_\mu \xi_+^{-1} \psi_+ \left(\xi_+ \partial_\mu \xi_+^{-1} \psi'_+ + \xi_- \partial_\mu \xi_-^{-1} \psi'_- \right) (1+z^2) \right]_{z=+\infty} \\ &\quad - \text{Tr} \left[\xi_- \partial_\mu \xi_-^{-1} \psi_- \left(\xi_+ \partial_\mu \xi_+^{-1} \psi'_+ + \xi_- \partial_\mu \xi_-^{-1} \psi'_- \right) (1+z^2) \right]_{z=-\infty}. \end{aligned} \quad (39)$$

Using the explicit expression for the modes ψ_\pm the boundary terms reduce to

$$S = \frac{1}{\pi} \int d^4x \text{Tr} \left[(\xi_+ \partial_\mu \xi_+^{-1} - \xi_- \partial_\mu \xi_-^{-1})^2 \right], \quad (40)$$

From this result we should now read off how to identify the ξ_\pm parameters with the pion $U = \exp i\pi$. There are many choices which one can make, but one useful one is $\xi_- = 1$ and $\xi_+ = U$ (note that for this particular gauge choice, the contribution from the $z = -\infty$ boundary is absent altogether). This leaves the chiral action

$$S = -\frac{1}{\pi} \int d^4x \text{Tr} \left[\partial_\mu U \partial_\mu U^{-1} \right]. \quad (41)$$

By also taking into account the commutator terms in the non-abelian field strength, one in fact recovers the full Skyrme action for the pions [36]. More importantly, the string dual also predicts how the Skyrme model pions should be coupled to an infinite tower of massive vector mesons.

Let us therefore continue with the massive meson modes. It is no longer possible to solve (35) analytically, but it is possible to obtain the solutions numerically. A Frobenius analysis shows that the asymptotic solution of (35) behaves, up to an overall normalisation, as

$$\psi(z) \sim \frac{1}{z} \left(1 + \frac{c_1}{z^{2/3}} + \frac{c_2}{z^{4/3}} + \dots \right), \quad (42)$$

where the first few coefficients c_i are given by

$$c_1 = -\frac{9}{10 u_0} (\omega^2 - \mathbf{k}^2), \quad c_2 = \frac{81}{280 u_0^2} (\omega^2 - \mathbf{k}^2)^2. \quad (43)$$

Using this as an initial condition at $z = -\infty$, solving the differential equation numerically and demanding normalisability at $z = +\infty$ then yields a discrete spectrum of masses, starting with [36]

$$(\omega^2 - \mathbf{k}^2)^{CP} = 0.67^{--}, 1.57^{++}, 2.87^{--}, 4.55^{++}, \dots, \quad (44)$$

in units of the single mass scale of the model. The parity and charge conjugation properties are also indicated. By generalising this analysis for arbitrary u_0 one can also compute the dependence of the masses on the quark masses m_q , see figure 9 (this relies on the relation between $u_0 - u_A$ and the constituent quark mass, which we will discuss in the next section).

It is tempting to compare these results to actual meson masses, and one finds that the ratios are in reasonable agreement with experiment. A similar agreement is found when the analysis is generalised to interactions of mesons [36]. The goal here is not so much to argue

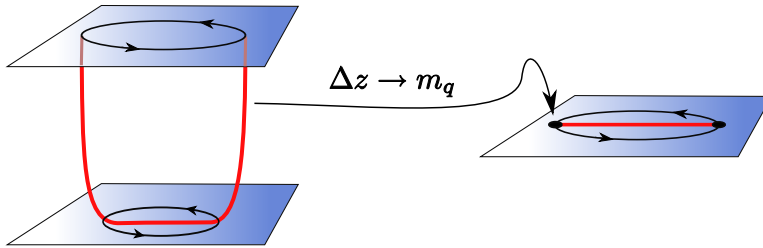


Fig. 10. A large-spin meson in the string/gauge theory description. The endpoints of the string map to the quark and anti-quark in the gauge theory picture, while the string between them extends deeply into the curved geometry. The masses of the quarks are now represented by the long vertical string segments [40].

that the string/gauge duality can pin down these numbers accurately (which it cannot), but rather to show that the model seems to capture some of the universal features which also make many other models get the numbers right. The exciting aspect is that this patterns follows from equations which at first sight have nothing to do with mesons.⁴

3.3 Long strings and hadron fragmentation

Let us now turn to large-spin mesons. These are described by long, U-shaped strings which hang from the flavour branes, with their end-points attached to it, as in figure 10. One can solve the equation of motion for such a string, and find the energy and angular momentum as a function of the separation L and the angular velocity ω ,

$$\begin{aligned}
 E &= 2 \frac{T_{\text{eff}}}{\omega} \left(\arcsin(\omega L) + \sqrt{\frac{m_q}{T_{\text{eff}} L}} \right), \\
 J &= \frac{T_{\text{eff}}}{\omega^2} \left(\arcsin(\omega L) + (\omega L)^2 \sqrt{\frac{m_q}{T_{\text{eff}} L}} \right).
 \end{aligned}
 \tag{45}$$

Intriguingly, by eliminating ω , one finds at leading order precisely the relation between energy and angular momentum for a relativistic four-dimensional string with massive endpoints [40]. The masses of the endpoints map to the masses of the vertical string segments. These stretch between the bottom of the flavour brane at $u = u_0$ and the bottom of the geometry at $u = u_\Lambda$, and thus

$$m_q = \frac{1}{2\pi\alpha'} \int_{u_\Lambda}^{u_0} \sqrt{-g_{tt}g_{uu}} du.
 \tag{46}$$

For large u_0 , and using the metric (25), this shows a simple linear relation between the constituent quark mass and the parameter u_0 .

In the real world, large-spin mesons are extremely unstable (the Particle Data Book lists decay rates only for spins to about 6; higher spin mesons decay too rapidly [10]). However, the situation is quite different in the large- N_c limit. As we have seen, this limit implies an arbitrarily

⁴ To be fair, there are also several qualitative aspects which the Sakai-Sugimoto model does not get right. It has an exotic 0^{++} state, but lacks J^{+-} states altogether. The mass of the pions (identically zero) is not related to the constituent quark masses (see however [39] for directions on how to cure this). The Kaluza-Klein modes on the sphere lead to a tower of modes which are not separated from the others by a large mass gap. As in all weakly curved models, there is a large gap between mesons of spin ≥ 1 and those of higher spin. Finally, because the supersymmetry breaking scale is of the order of the meson mass scale, there is a whole tower of fermionic mesons which are partners of the bosonic ones; these are obviously also not present in QCD.

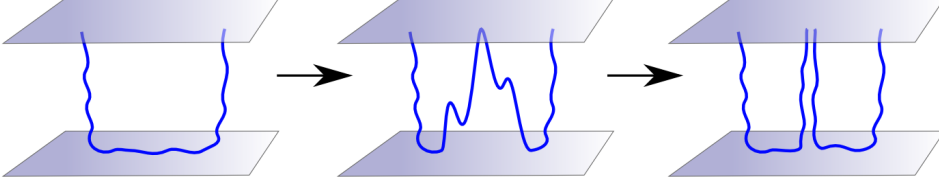


Fig. 11. A fluctuating string may touch a flavour brane, at which point it can split and reconnect, thus resulting in two open strings.

small string coupling constant, and decay processes are suppressed by at least one power of N_c . Therefore, it makes sense to study decaying large strings in the string/gauge theory duality.

Moreover, there is reasonable evidence for the existence of short-lived large-spin mesons in a more indirect form. In any particle collider, after one leaves the hard, perturbative regime, one enters a stage in which the quarks and leptons that have been produced combine and form hadrons. This hadronisation stage is not understood from first principles, but several Monte-Carlo tools for the analysis of collider data are based on phenomenological string breaking models such as the Lund model [41, 42]. Although the large-spin mesons are too short-lived to be seen directly, one does observe the decay products; the fact that programs such as PYTHIA reproduce collider data so far quite well lends support to the idea that large-spin mesons really do exist.

One of the more popular phenomenological models for large-spin meson decays is the CNN model [43]. It is based on the idea of modelling the force between the quarks in a meson by a chromoelectric flux tube. The probability of such a meson decaying is then directly related to the probability of creating a new quark/anti-quark pair inside the flux tube. This probability is the standard Schwinger pair production probability, given by the characteristic exponential suppression factor

$$P_{\text{pp}} = \exp\left(-\frac{\pi m_q^2}{2 T_{\text{eff}}}\right) \rightarrow P = \frac{T_{\text{eff}}^2}{\pi^3} \sum_{n=1}^{\infty} \frac{1}{n^2} \exp\left(-\frac{\pi n m_q^2}{2 T_{\text{eff}}}\right) \quad (47)$$

The decay width is then given by multiplying this with the volume of the flux tube,

$$\Gamma = L \cdot \pi r_t^2 P = L \cdot T_{\text{eff}} (\text{number}) \sum_{n=1}^{\infty} \frac{1}{n^2} \exp\left(-\frac{\pi n m_q^2}{2 T_{\text{eff}}}\right) \quad (48)$$

For vanishing quark masses, we find that the decay width divided by the total mass is a constant, because the mass of the flux tube is also linear in L ,

$$m_q = 0 \rightarrow M = T \cdot L \rightarrow \frac{\Gamma}{M} = \text{const.} \quad (49)$$

When the quark masses are non-zero we have, for a fixed total mass, a shorter flux tube,

$$\frac{L}{M} = \frac{2}{\pi T_{\text{eff}}} - \frac{m_1 + m_2}{2T_{\text{eff}}M} + \mathcal{O}\left(\frac{m_i^2}{M^2}\right). \quad (50)$$

This results in Γ/M versus M plots not being straight lines [44].

The string/gauge theory correspondence claims to give a more fundamental link between mesons and long strings. The question is thus whether the results of the CNN model can be reproduced from the string/gauge theory correspondence. The first thing to note is that fundamental quarks are no longer present, but their masses are a reflection of the masses of

the vertical segments of the U-shaped string. Instead of pair-creating quarks, we should thus consider processes which lead to new vertical segments.

Now the U-shaped string is a quantum object, and this implies that it fluctuates. In fact, it is possible for the horizontal part of the string to fluctuate up to a flavour brane, as in figure 11. If that happens, the point at which the string touches the flavour brane can split and the two new endpoints can reconnect to the brane. This leads to two U-shaped strings, and therefore our original meson has decayed into two new mesons.

The probability for this process to happen can be calculated, at least in the approximation where the gravitational field is approximately constant between the bottom of the space-time (the “infrared wall”) and the flavour brane. The splitting probability is a product,

$$\mathcal{P} = \mathcal{P}_{\text{fluctuate}} \times \mathcal{P}_{\text{split}}. \quad (51)$$

The first factor describes the probability for the string to fluctuate to the flavour brane, while the second factor describes the probability that it will actually split there. The second factor has to do with a process which takes place on the flavour brane, where the curvature is constant. Therefore, we can use standard flat-space results for this. The first factor, on the other hand, requires precise control over the wave function of the string.

Recall how this is done in flat space. The Polyakov action for the string in flat space is given by

$$S = \int d\tau d\sigma (\dot{X}^2 - X'^2) \quad \rightarrow \quad S = \int d\tau \sum_n (\dot{a}_n^2 - \omega_n^2 a_n^2), \quad (52)$$

where we have decomposed in Fourier modes. The wave function is a function over the variables a_n , i.e.

$$\Psi[\{a_n\}] = \prod_n \Psi_n[a_n(X)], \quad (53)$$

where all the Ψ_n are harmonic oscillator wave functions. If we put all oscillators in the ground state, we end up with

$$\Psi_n[a_n] \sim \exp\left(-\omega_n a_n^2\right). \quad (54)$$

In curved space, the logic is the same, only the mode expansions become more complicated. One has to find fluctuations around the U-shaped string which are such that the action decouples as a sum of normal modes, with coefficients η_n , like in (52). The upshot is that the wave function now takes the form

$$\Psi[\{\eta_n\}] = \prod_n \Psi_n[\eta_n(X)]. \quad (55)$$

The goal is then to compute the total probability that the string touches the flavour brane, i.e. compute the integral

$$\Gamma = T_{\text{eff}} \mathcal{P}_{\text{split}} \times \int_{\{\eta_n\}} |\Psi[\{\eta_n\}]|^2 K[\{\eta_n\}], \quad (56)$$

where we integrate over all configurations such that the string touches the flavour brane with at least one point. The factor $K[\{\eta_n\}]$ is a measure factor with the dimension of length. It measures, for a given string configuration, the size of the segment(s) of the string which intersect(s) the flavour brane. This is a tricky computation because of the boundary conditions. However, various estimates and a computation using a string bit model agree on the result [45]. Namely, one indeed finds that the decay width is close to a Gaussian in the distance to the flavour brane, or in terms of gauge theory variables, a Gaussian in m_q (see figure 12). One finds precisely the CNN result (48).

Interestingly, one can go beyond the approximation of flat space and try to take into account the curvature of the background. This should encode possible corrections to the Lund decay

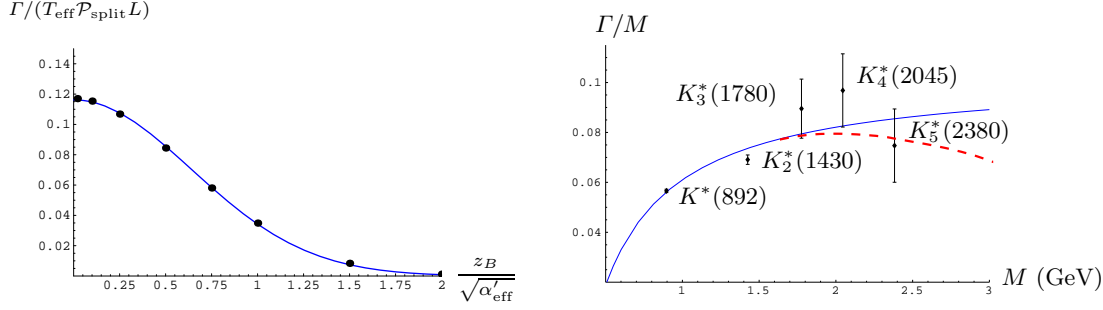


Fig. 12. The decay width per unit length for a meson computed using a holographic dual (left). Corrections from the curvature of the background generically predict that the decay widths are suppressed for very large spins, which is symbolically depicted in the plot for the K^* decay widths on the right (the continuous, blue curve is the leading order result on which the CNN model and the holographic computation agree).

widths. For the model at hand, the wave functions can be computed analytically in terms of Mathieu functions; the upshot is that the wave function for the n -th mode becomes

$$\Psi[\eta_n] \sim \exp \left[-\frac{2}{3\alpha'} (R_{D4}^3 u_\Lambda)^{1/2} (a_n(b/2) + b)^{1/2} \eta_n^2 \right] \quad \text{where} \quad b = \frac{27}{4} \pi^2 \frac{J}{g_{YM}^2 N_c} + \dots, \quad (57)$$

where $a_n(b)$ are the Mathieu characteristic functions which at leading order in b behave as n^2 (b is given in the approximation where the quarks are light). In this model, and various related ones, we thus conclude that the generic trend is for curvature effects to suppress the decay of mesons with very large spin [45].

4 Finite temperature and phase transitions

4.1 Temperature and Euclidean geometry

Much of the interest in the string/gauge theory correspondence comes from applications to finite-temperature physics. Before we can discuss string duals to gauge theories at finite temperature, let us first recall how black holes are related to finite temperature. The simplest way to see this, and the way which connects most straightforwardly to what we will say later, is to look at the Euclidean section of a black hole geometry. If we start from the Schwarzschild geometry and perform a Wick rotation $t = i\tau$, we end up with the geometry

$$ds^2 = \left(1 - \frac{2m}{r}\right) dt^2 + \left(1 - \frac{2m}{r}\right)^{-1} dr^2 + r^2 d\Omega^2. \quad (58)$$

If we now introduce a new coordinate $\tilde{r} = r - 2m$ and then $\rho^2 = 8m\tilde{r}$, we end up very close to the horizon $r = 2m$ with the metric

$$ds^2 = \frac{\tilde{r}}{2m} dt^2 + \frac{2m}{\tilde{r}} d\tilde{r}^2 + 4m^2 d\Omega^2 = \left(\frac{\rho}{4m}\right)^2 dt^2 + d\rho^2 + 4m^2 d\Omega^2. \quad (59)$$

In the ρ, t subspace, this is precisely a flat metric in polar coordinates, with t playing the role of the angular coordinate. We thus see that we naturally get a compactified Euclidean time. In order to identify the period, note that unless we identify $t \sim t + 2\pi \cdot 4m$, this metric will exhibit a conical singularity. Therefore, we choose this particular size of the Euclidean circle, and end up with a temperature

$$T = \frac{1}{8\pi m}. \quad (60)$$

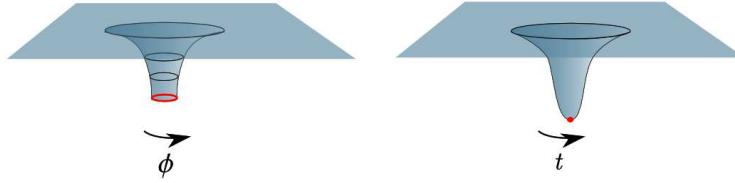


Fig. 13. Lorentzian versus Euclidean sections of the Schwarzschild geometry. In the Euclidean section, the circle spanned by the t coordinate shrinks to zero size at the horizon, leaving a conical singularity unless $t \sim t + 2\pi \cdot 4m$.

This is precisely the temperature that can also be obtained by using Hawking's original derivation of the temperature of radiation produced by a black hole. The difference between the Lorentzian and Euclidean black hole geometry is once more visualised in figure 13.

Let us now look at the thermal characteristics of the string geometries that play a role in the string/gauge theory correspondence. The first metric which we encountered was the one of AdS_5 . After a Wick rotation, it can be written in the form

$$ds_{\text{AdS}_5}^2 = \left(1 + \frac{r^2}{R^2}\right) dt^2 + \left(1 + \frac{r^2}{R^2}\right)^{-1} dr^2 + r^2 d\Omega_3^2. \quad (61)$$

This metric is regular everywhere for any radius of the time-like circle, i.e. $t \sim t + \beta$ for any arbitrary β . However, there exists another solution to the supergravity equations of motion, with the same asymptotic geometry $S^1 \times S^3$, whose Euclidean section takes the form

$$ds_{\text{AdS-BH}_5}^2 = \left(1 + \frac{r^2}{R^2} - \frac{\mu}{r^2}\right) dt^2 + \left(1 + \frac{r^2}{R^2} - \frac{\mu}{r^2}\right)^{-1} dr^2 + r^2 d\Omega_3^2. \quad (62)$$

This is the so-called AdS_5 black hole, and this geometry has a horizon (in the Lorentzian section) at

$$r^2 = r_+^2 = (R/2)(-R + \sqrt{R^2 + 4\mu^2}). \quad (63)$$

Moreover, with an identification $t \sim t + \beta$ the geometry has a conical singularity unless

$$\beta = \frac{4\pi R^2 r_+}{4r_+^2 + 2R^2}. \quad (64)$$

This fixes the temperature of the black hole.

The two geometries (61) and (62) compete with each other in the Euclidean partition sum,

$$Z = \sum_{\text{configurations}} \exp[-\beta F]. \quad (65)$$

where F is the free energy, related to the Euclidean action by $S_E = \beta F$. The dominant one is the one with smallest Euclidean action. One can compute this action explicitly [27], but the details are not important. The phase diagram of this system is rather simple because there is only one parameter (the temperature) to vary. One finds that below a certain critical temperature, the dominant configuration is (61), while above this temperature, the partition sum is dominated by the black hole (62).⁵

⁵ To be precise, there are always two black hole geometries competing in the partition sum, since at a fixed temperature there are two solutions of (64) for r_+ . The one which dominates at large temperature is the one with the largest value of r_+ .

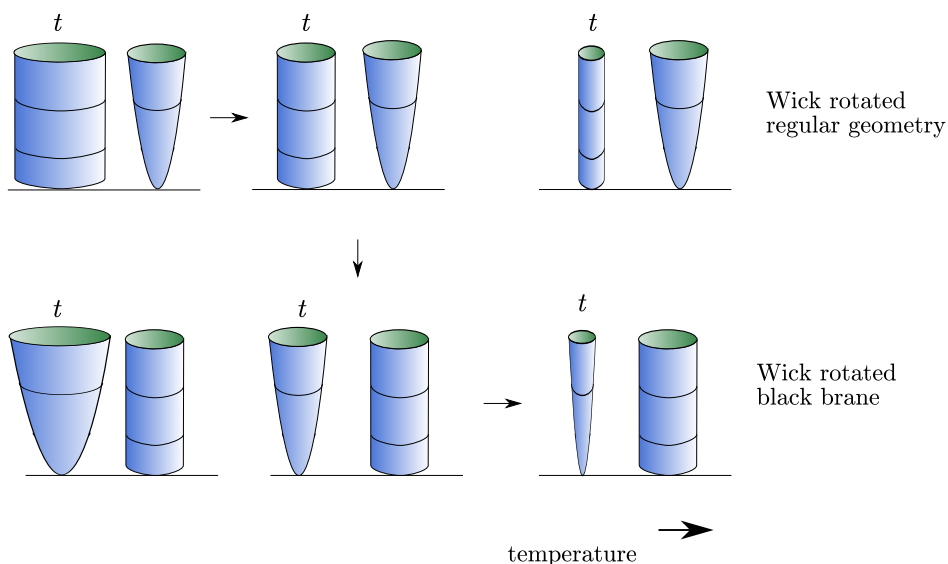


Fig. 14. The two D4-brane based geometries which compete in the Euclidean partition sum: both are described by the same metric (66), the difference is only which circle changes size as we change the temperature. For the regular geometry, temperature is related to the size of the cylinder, while for the black hole geometry, temperature is related to the radius of the cigar.

4.2 Phase diagrams

The phase diagram for the $N = 4$ theory as we discussed above is not particularly realistic, as it does not exhibit confinement and also does not contain any quark degrees of freedom. We can use it as a guideline, however, to study more realistic gauge theories, such as the confining model discussed in section 3.1. If we Wick rotate the metric (25) we end up with

$$ds^2 = \left(\frac{u}{R_{D4}}\right)^{3/2} [dt^2 + \delta_{ij}dx^i dx^j + f(u)d\theta^2] + \left(\frac{R_{D4}}{u}\right)^{3/2} \left[\frac{du^2}{f(u)} + u^2 d\Omega_4\right] \quad (66)$$

One feature which sets this metric apart from the Euclidean ones we have seen so far is that it contains *two* circles. One is the circle spanned by the θ coordinate, with period L_A (see (27)), which was also present in the Lorentzian geometry. The other one is the new Euclidean time-like circle spanned by t .

We could therefore wonder whether we could perhaps view θ as the thermal circle? If we Wick rotate back, but now on the θ coordinate, we end up with a metric which near $u = u_A$ takes the form

$$-f(u)d\theta^2 + (\dots)du^2 + \delta_{ij}dx^i dx^j. \quad (67)$$

Recalling that $f(u) = 1 - u_A^3/u^3$, this metric is very much like a black hole metric, with a horizon at $u = u_A$ and a temperature given by $T = L_A^{-1}$. We thus have access to two different thermal interpretations of the Euclidean metric (66), one based on a regular Lorentzian geometry in which t is the Euclidean time, and one based on a Lorentzian black hole (or rather “black brane”) geometry in which θ is the Euclidean time.

In the Euclidean partition sum for quantum gravity, these two configurations again compete, and the one with smallest action will dominate at a given temperature. This balance is sketched in figure 14. At low temperatures, the dominating geometry turns out [46] to be the regular one (with a large radius cylinder factor and a fixed-radius cigar). As we decrease the radius of the cylinder, we encounter a point where the radius is equal to that of the cigar. At this

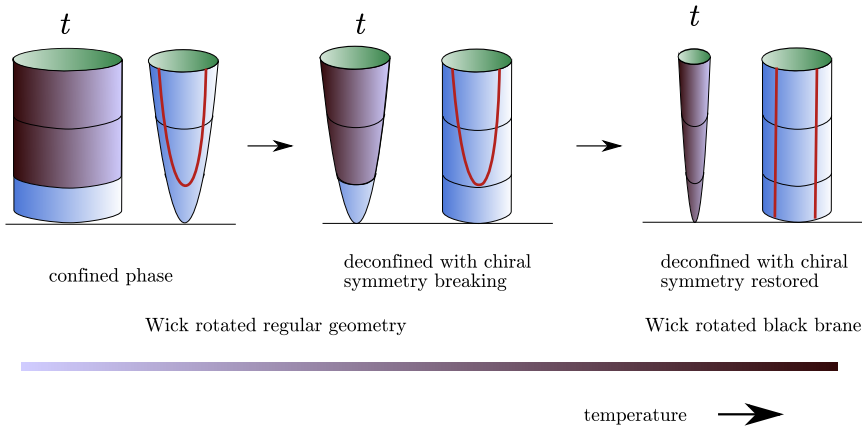


Fig. 15. The three possible phases of the Sakai-Sugimoto model, showing the two background geometries (regular or black) and the two possible brane embeddings (connected or disconnected).

point, the Wick rotated black hole phase takes over. This transition is first-order because the solutions do not smoothly connect, and continue to exist as separate solutions both below and above the transition. The spectrum of the glueball fluctuations in the phase described by (67) is *continuous*, signalling the deconfinement of the gluonic degrees of freedom.

An order parameter of this phase transition is the Polyakov loop, corresponding to a string wrapped around the time direction. In the low-temperature phase the time circle is non-contractible and not the boundary of a disc, so that the Polyakov loop vanishes. After the transition, this circle becomes contractible, resulting in a non-zero expectation value for the Polyakov loop. Other order parameters are the Wilson loop (which has a linear quark/anti-quark potential in the first background but vanishing tension in the second) and the behaviour of the free energy as a function of N_c (namely $\sim N_c^0$ for the first background and $\sim N_c^2$ for the second), and the presence of a glueball spectrum with a mass gap.

Just as at zero temperature (discussed in section 3.2), we can now add flavour D8-branes to the system. This is depicted in figure 15. The D8-brane always wraps the Euclidean time circle, and describes a curve in the subspace described by the other circle and the u direction. At low temperatures, the branes are connected, leading to chiral symmetry breaking as discussed in section 3.2. Once in the black hole phase, however, there comes a temperature at which it is energetically more favourable for the D8-branes to disconnect and go vertically down to the horizon. Chiral symmetry is restored here.

Whether or not the intermediate phase, which has deconfined gluons but confined mesons, exists depends on the masses of the constituent quarks. The phase diagram of the model is given in figure 16 [46].

4.3 Mesons and meson melting

In the intermediate-temperature phase, in which there is a black brane background encoding the dynamics of deconfined gluons, there may still be bound states of the matter degrees of freedom. In order to analyse these, one needs to analyse the dynamics of the flavour brane in the black brane background. Just as before, there are low-spin massive vector mesons described by the small fluctuations of the gauge fields on the flavour brane. The thermal (pole) masses, defined for homogeneous modes by

$$\partial_0^2 B_i^{(n)} = -m_n^2 B_i^{(n)}, \quad (68)$$

can be computed by solving a fluctuation equation similar to the zero-temperature case displayed in (35). It now reads

$$-u^{1/2} \gamma^{-1/2} f(u)^{1/2} \partial_u \left(u^{5/2} \gamma^{-1/2} f(u)^{1/2} \partial_u \psi_{(n)} \right) = R_{D4}^3 m_n^2 \psi_{(n)}. \quad (69)$$

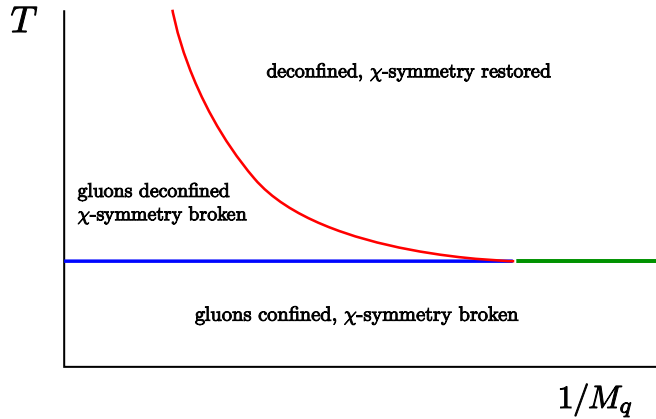


Fig. 16. The phase diagram for the Sakai-Sugimoto model [46]. For large enough constituent quark masses, one encounters three phases as the temperature is increased: starting with a fully confined phase, first the gluons deconfine, and later the chiral symmetry gets restored and mesons deconfine too. For smaller quark masses the deconfinement goes in one step.

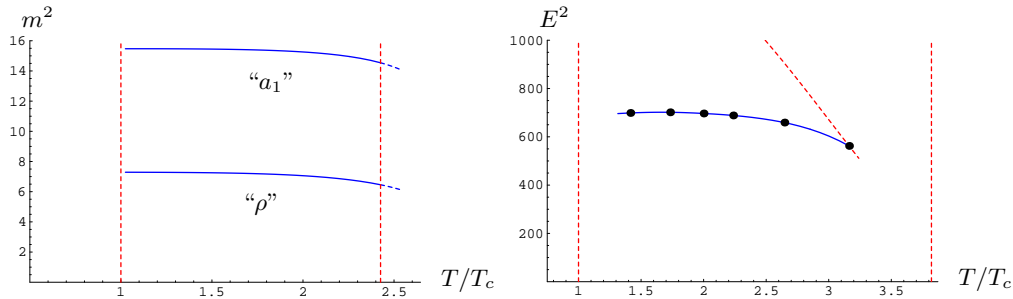


Fig. 17. The behaviour of the masses of small-spin mesons (left) and large-spin mesons (right) as a function of temperature. While small-spin mesons survive all the way up to the transition into the high-temperature phase, large-spin mesons cease to exist beyond a certain temperature, when they get too close to the horizon and disappear from the spectrum.

The only difference is the insertion of two extra factors $\sqrt{f(u)}$. The spectrum remains discrete, labelled by the mode number n and parity. By keeping the asymptotic geometry fixed, including the separation L between the flavour branes, and changing the temperature, one can determine the behaviour of the masses as a function of temperature.

By comparing with the zero-temperature result, one observes that the masses of light mesons decrease as the temperature is increased [47]. The temperature dependence of the masses of the “ ρ ” and “ a_1 ” mesons are shown on the left panel of figure 17. These mesons survive all the way up to the transition into the phase where chiral symmetry is restored. Large-spin mesons, on the other hand, can be shown to disappear from the spectrum once they reach a certain critical size; see the right panel of figure 17.

These findings are in qualitative agreement with lattice computations [48, 49], although the Sakai-Sugimoto model does not exhibit the degeneracy of the ρ and a_1 meson masses at high temperature. Moreover, we will see below that the spectrum becomes continuous in the phase where chiral symmetry is restored. Therefore, the phase transition from intermediate to high temperature, which is first-order in our model, is rather different from the one in QCD. However, what we see is consistent with the fact that mesons in the chirally symmetric phase are extremely unstable in the large- N_c limit: their decay widths scale as a positive power of N_c .

Finally, let us briefly discuss the high-temperature phase. In this phase, the minimal free energy of the system is attained when the two stacks of branes are disconnected (see the

third panel of figure 15). The profile of the left and right stacks of branes is characterised by $u' \equiv du/d\theta \rightarrow \infty$. The differential equation for the modes, analogous to (35) and (69) for the other two phases, is now

$$-u^{1/2} f(u)^{1/2} \partial_u \left(u^{5/2} f(u)^{1/2} \partial_u \psi_{(n)} \right) = R_{D4}^3 m_n^2 \psi_{(n)}. \quad (70)$$

which differs from the one at intermediate temperature (69) by the absence of the γ factors.

In this phase, the massless pion disappears from the spectrum. The reason is that this mode, which would be given by $\phi^{(0)} = u^{-5/2} f(u)^{-1/2}$, is no longer normalisable. The norm compatible with the differential equation (70) leads, for the would-be pion mode, to the divergent integral

$$\int_{u_T}^{\infty} du u^{5/2} f(u)^{-1/2} \left| u^{-5/2} f(u)^{-1/2} \right|^2. \quad (71)$$

Although this integral is convergent at the upper boundary, it diverges at the lower boundary because $f(u) \sim \sqrt{u - u_T}$ for $u \sim u_T$. The crucial ingredient is that the D8-branes extend all the way down to the horizon at $u = u_T$, which did not happen in the intermediate temperature phase. Thus, in accordance with the fact that chiral symmetry is restored in the high-temperature phase, we see that the Goldstone boson has disappeared. The remainder of the spectrum turns out to be continuous.

5 Using strings to study the quark-gluon fluid

Given that string duals to gauge theories are computationally tractable only when the 't Hooft coupling is large, it is only natural that new observed gauge theory phenomena at strong coupling would catch the interest of string theorists. The discovery of the strongly coupled quark gluon fluid at RHIC thus came as a nice surprise not only for experimentalists [50].

One of the first properties of the fluid which caught the attention is its low viscosity [51]. Using the string theory dual of gluon fluids, this turned out to have an extremely natural interpretation in terms of properties of black hole horizons. An excellent review article of this topic has meanwhile appeared [52], so we will refrain from discussing this issue here in detail. Instead, we will focus on two other applications which are of a more recent nature, namely the study of drag forces and the study of screening lengths. These both involve the dynamics of quarks inside the deconfined gluon fluid, and require an intermediate temperature phase as we have seen in previous sections.

5.1 Drag forces and jet quenching

When a quark/anti-quark pair is produced inside a particle collider, the quark and anti-quark will typically end up hadronising into back-to-back jets. However, when pair production takes place inside the quark-gluon fluid, and the pair is produced close to the boundary of the fluid ball, the situation is different. One of the quarks will be able to escape the fluid and form a jet as usual, but the other quark has to travel a long way to the other side of the fluid and will lose energy in this process. The result is a signal with one well-defined jet and a much smeared-out signal on the other side of the detector. This phenomenon, known as “jet quenching”, thus tells us something about the interaction of the fluid with the quarks. From Bremsstrahlung-type calculations one can estimate the energy loss which quarks experience at weak coupling. At strong coupling, the drag force can be computed using the string/gauge theory correspondence [53, 54].

The main ingredient is that a single quark can be modelled by a string ending on a flavour brane and hanging down all the way to the horizon. We thus use a stationary ansatz for the string of the form

$$x(u, t) = vt + x(u). \quad (72)$$

The computation was originally done for an AdS₅ black hole with flat horizon, but can easily be extended to more complicated metrics. For an ansatz of the form above, the action of the string reduces to

$$S_{\text{string}} = \int d\tau d\sigma \sqrt{-g} = \int d\tau d\sigma \sqrt{-g_{tt}g_{xx}(x')^2 - g_{tt}g_{uu} - g_{xx}g_{uu}v^2}. \quad (73)$$

Since there is no explicit x -dependence, the equation of motion is given by a simple ordinary differential equation, which can be integrated once trivially; making use of (73) we find

$$\frac{d}{du} \left(\frac{g_{tt}g_{xx}}{\sqrt{-g}} \frac{d}{du} x(u) \right) = 0 \quad \rightarrow \quad (x(u)')^2 = \frac{C^2(-g_{tt}g_{uu} - g_{xx}g_{uu}v^2)}{g_{tt}g_{xx}(g_{tt}g_{xx} + C^2)}. \quad (74)$$

As we have seen twice in a different situation, we will not need more than the derivative x' in order to find the drag force. Substituting the result for x' back into the action, the result is

$$S_{\text{string}} = \int d\tau d\sigma \sqrt{-\frac{g_{tt}g_{uu}g_{xx}(g_{tt} + g_{xx}v^2)}{C^2 + g_{tt}g_{xx}}}. \quad (75)$$

This expression tells us how to determine the constant C . If we do not choose it appropriately, the string will reach a point $u = u_c$ where the numerator inside the square root will change sign. This happens at $g_{tt} + g_{xx}v^2 = 0$, which is a point *above* the horizon, which is located at $g_{tt} = 0$. Clearly, a physical solution cannot have imaginary action. Therefore, a solution which reaches $u = u_c$ will have to have its C chosen such that the denominator changes sign here too. After C has been fixed in this way, the shape of the string can always be found by integrating (74) once more, if necessary numerically.

However, in order to determine the drag force which has to be exerted on the string, we do not need to know the shape $x(u)$. We merely have to compute the momentum density

$$P^1_x := \frac{\delta S}{\delta x(u)'} = -\frac{1}{2\pi\alpha'} \frac{g_{tt}g_{xx}x(u)'}{\sqrt{-g}}. \quad (76)$$

The force at the endpoint is related to this by $F = dp_x/dt = \sqrt{-g}P^1_x$. For the Sakai-Sugimoto model, this calculation leads to [55]

$$F_{\text{drag}} = -\frac{1}{2\pi l_s^2} \frac{v}{\sqrt{1-v^2}} \left(\frac{u_A}{R_{\text{D4}}} \right)^{3/2} = -\frac{1}{2\pi} \frac{v}{\sqrt{1-v^2}} \left(\frac{4\pi}{3} \right)^3 \lambda_4 T^2, \quad (77)$$

where use was made of the expression for the temperature in terms of the circle radius, $T = L_A^{-1}$ together with (27) and the expression for the four-dimensional 't Hooft coupling (28). Note that there is no explicit power of N_c^2 here, so this expression does not scale as the entropy density s or as a power of the energy density $\epsilon^{3/4}$. The result is also independent of the quark mass. If required this drag force can be used to compute the “jet quenching parameter” [53].

These calculations can of course be repeated for other non-conformal gravity duals [56] as well as for backgrounds modified by α' corrections [57], with qualitatively similar results. In contrast to the entropy bound, however, the drag force is not universal for all gauge theories which have a gravity dual (neither the numerical coefficients nor the behaviour as a function of the 't Hooft coupling are the same for all gauge theories with string duals).

5.2 Screening length

The last topic we will discuss is the computation of the screening length of the colour force in a strongly-coupled gluon fluid. From lattice calculations, it is now known that the quark/anti-quark potential starts to flatten out when the separation exceeds a certain temperature-dependent scale L_s . By dimensional reasoning one expects $L_s \sim 1/T$, and explicit computations fix the proportionality constant; see e.g. [58].

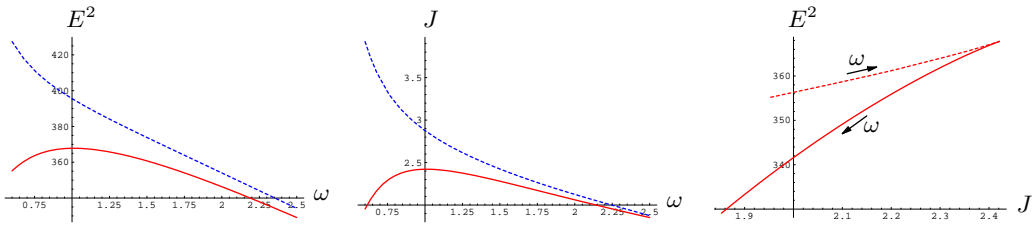


Fig. 18. The energy (squared) and angular momentum of U-shaped strings, as a function of the frequency ω . The dashed (blue) curves are for zero temperature, while the solid (red) curves are for the intermediate-temperature regime.

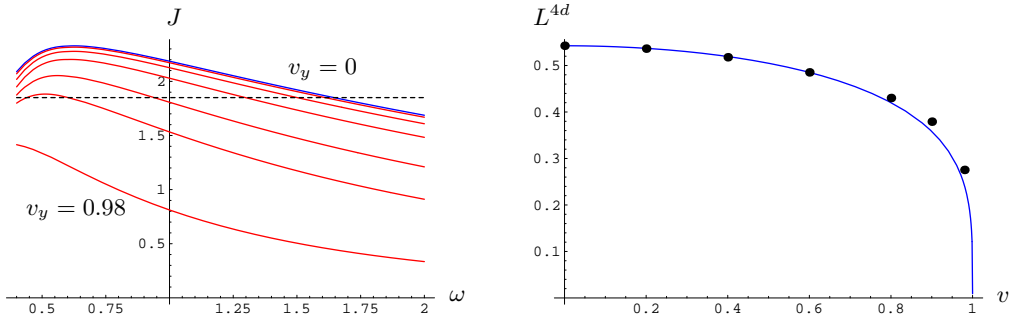


Fig. 19. The behaviour of the spin J as a function of the angular and transverse velocities ω and v_y respectively (left). The size of the maximum-spin meson depends on v_y . This leads to a plot of the four-dimensional size L^{4d} for maximum-spin mesons as a function of the transverse velocity (right). The blue curve depicts the relation $L^{4d}(v=0) \cdot (1-v^2)^{1/4}$, as obtained analytically for Wilson loops in [59].

In order to apply this result to dynamical situations occurring in the strongly-coupled quark gluon fluid, one would need to know the behaviour of the screening length when the quark/anti-quark pair is not at rest with respect to the medium, but has a non-zero velocity. This is much harder to do on the lattice as it involves time-dependence at finite temperature. However, as the drag force calculation shows, the string/gauge theory correspondence has the potential to deal with such time-dependent finite temperature situations efficiently.

The situation we need to study is that of a large-spin meson, for which we want to know the maximum possible size as a function of the temperature and the velocity with respect to the medium. In the Sakai-Sugimoto background these rotating mesons can be obtained numerically [47] both at zero and at finite temperature. These colour-singlet states do not experience a drag force like the isolated quarks do, because the string stretching between the quarks never reaches the horizon. From the field-theoretic point of view this makes sense, as the absence of a colour monopole moment means that these states do not couple directly to gluon degrees of freedom. Because of the absence of drag, mesons do not experience any energy loss when propagating through the quark-gluon fluid: no force is necessary to keep them moving with fixed velocity. However, their shape is certainly velocity dependent. For higher velocity, the distance to the horizon decreases, leading to a lower melting temperature.

To make this more precise, let us plot the energy and angular momentum as a function of the angular velocity ω (see figure 18). When we eliminate the variable ω from the left and middle plots in figure 18, we obtain the plot on the right, expressing the energy versus the spin. The appearance of a maximum in energy and spin is clearly visible. We also see that the two states with identical spin J actually have different energy: the ones with smaller ω are more energetic than the ones with larger ω . Therefore, the upper branch to the left of the maxima in the plots of figure 18 is presumably unstable and will decay to the lower branch.

These curves can be analysed also for various values of the transverse velocity v . This yields the left plot in figure 19. From this plot we see that for a fixed temperature there is a *maximal* value of the spin which a meson can carry. It is natural to interpret the temperature at which this happens as the critical temperature at which a meson of spin J_{\max} melts. Thus we conclude that (as intuitively expected) the dissociation temperature of large-spin mesons is *spin dependent*. As the temperature increases, the maximal value of the spin that a meson can carry decreases, i.e. for given quark mass, higher-spin mesons melt at lower temperature. There is thus a critical velocity beyond which a meson of fixed spin has to dissociate. Similarly, the four-dimensional size of the meson decreases with increasing velocity. The data is approximated rather well [47] by the relation

$$L_{\max\text{-spin}}^{4d}(v) \approx L_{\max\text{-spin}}^{4d}(v=0) \cdot (1-v^2)^{1/4}. \quad (78)$$

This fit was motivated by the analytic results of [59], in which a similar dependence on the velocity was found for the screening length, or more precisely, the maximum interquark distance for Wilson loops in an AdS black hole background. See also related results in [60].

6 Conclusions

We have reviewed how the “new” string description of gauge theories has led to several intriguing results about strong-coupling gauge theory dynamics, with interesting connections to RHIC physics. Although we still lack a proper proof of the string/gauge theory correspondence (even in the prototype AdS/CFT case), it has certainly already led to a fascinating geometrical point-of-view on many problems which are hard to tackle with lattice or effective field theory models. It will be interesting to see how this new approach continues to complement other theoretical tools in the future.

Acknowledgements

We thank Ofer Aharony and Cobi Sonnenschein for an inspiring collaboration on many of the topics discussed in this review and for feedback on the first draft. We would also like to thank the organisers of the 45th Winter School on Theoretical Physics in Schladming for the invitation to present these lectures, and the audience for many interesting comments and discussions. The work of KP was partially supported by VIDI grant 016.069.313 from the Dutch Organisation for Scientific Research (NWO).

References

1. J. M. Maldacena, “The large- N limit of superconformal field theories and supergravity”, *Adv. Theor. Math. Phys.* **2** (1998) 231–252, [hep-th/9711200](#).
2. A. M. Polyakov, “String theory and quark confinement”, *Nucl. Phys. Proc. Suppl.* **68** (1998) 1–8, [hep-th/9711002](#).
3. J. Polchinski, “Dirichlet-branes and Ramond-Ramond charges”, *Phys. Rev. Lett.* **75** (1995) 4724, [hep-th/9510017](#).
4. J. Kuti, “Lattice QCD and string theory”, *PoS LAT2005* (2006) 001, [hep-lat/0511023](#).
5. B. Muller and J. L. Nagle, “Results from the relativistic heavy ion collider”, *Ann. Rev. Nucl. Part. Sci.* **56** (2006) 93–135, [nucl-th/0602029](#).
6. N. Beisert, “The dilatation operator of $N = 4$ super Yang-Mills theory and integrability”, *Phys. Rev.* **405** (2005) 1–202, [hep-th/0407277](#).
7. G. 't Hooft, “A planar diagram theory for strong interactions”, *Nucl. Phys.* **B72** (1974) 461.
8. R. Gopakumar, “From free fields to AdS”, *Phys. Rev.* **D70** (2004) 025009, [hep-th/0308184](#).
9. F. Wilczek, “Diquarks as inspiration and as objects”, [hep-ph/0409168](#).
10. S. Eidelman et al., “Review of Particle Physics”, *Physics Letters B* **592** (2004) 1.
11. E. S. Fradkin and A. A. Tseytlin, “Nonlinear electrodynamics from quantized strings”, *Phys. Lett.* **B163** (1985) 123.
12. G. T. Horowitz and A. Strominger, “Black strings and p -branes”, *Nucl. Phys.* **B360** (1991) 197–209.
13. S. S. Gubser, I. R. Klebanov, and A. M. Polyakov, “Gauge theory correlators from non-critical string theory”, *Phys. Lett.* **B428** (1998) 105–114, [hep-th/9802109](#).
14. E. Witten, “Anti-de Sitter space and holography”, *Adv. Theor. Math. Phys.* **2** (1998) 253–291, [hep-th/9802150](#).
15. D. Z. Freedman, S. D. Mathur, A. Matusis, and L. Rastelli, “Correlation functions in the CFT(d)/AdS($d + 1$) correspondence”, *Nucl. Phys.* **B546** (1999) 96–118, [hep-th/9804058](#).
16. O. Aharony, S. S. Gubser, J. M. Maldacena, H. Ooguri, and Y. Oz, “Large- N field theories, string theory and gravity”, *Phys. Rev.* **323** (2000) 183–386, [hep-th/9905111](#).
17. D. T. Son and A. O. Starinets, “Minkowski-space correlators in AdS/CFT correspondence: recipe and applications”, *JHEP* **09** (2002) 042, [hep-th/0205051](#).
18. C. Csaki, H. Ooguri, Y. Oz, and J. Terning, “Glueball mass spectrum from supergravity”, *JHEP* **01** (1999) 017, [hep-th/9806021](#).
19. R. de Mello Koch, A. Jevicki, M. Mihailescu, and J. P. Nunes, “Evaluation of glueball masses from supergravity”, *Phys. Rev.* **D58** (1998) 105009, [hep-th/9806125](#).
20. J. M. Maldacena, “Wilson loops in large- N field theories”, *Phys. Rev. Lett.* **80** (1998) 4859–4862, [hep-th/9803002](#).
21. Y. Kinar, E. Schreiber, and J. Sonnenschein, “ $Q\bar{Q}$ potential from strings in curved spacetime – classical results”, *Nucl. Phys.* **B566** (2000) 103–125, [hep-th/9811192](#).
22. J. Polchinski and M. J. Strassler, “Hard scattering and gauge/string duality”, *Phys. Rev. Lett.* **88** (2002) 031601, [hep-th/0109174](#).
23. J. Erlich, E. Katz, D. T. Son, and M. A. Stephanov, “QCD and a holographic model of hadrons”, *Phys. Rev. Lett.* **95** (2005) 261602, [hep-ph/0501128](#).
24. G. F. de Teramond and S. J. Brodsky, “The hadronic spectrum of a holographic dual of QCD”, *Phys. Rev. Lett.* **94** (2005) 201601, [hep-th/0501022](#).
25. U. Gursoy and E. Kiritsis, “Exploring improved holographic theories for QCD: Part I”, [arXiv:0707.1324 \[hep-th\]](#).
26. U. Gursoy, E. Kiritsis, and F. Nitti, “Exploring improved holographic theories for QCD: Part II”, [arXiv:0707.1349 \[hep-th\]](#).
27. E. Witten, “Anti-de Sitter space, thermal phase transition, and confinement in gauge theories”, *Adv. Theor. Math. Phys.* **2** (1998) 505, [hep-th/9803131](#).
28. I. R. Klebanov and A. A. Tseytlin, “Entropy of Near-Extremal Black p -branes”, *Nucl. Phys.* **B475** (1996) 164–178, [hep-th/9604089](#).

29. N. Itzhaki, J. M. Maldacena, J. Sonnenschein, and S. Yankielowicz, “Supergravity and the large- N limit of theories with sixteen supercharges”, *Phys. Rev.* **D58** (1998) 046004, [hep-th/9802042](#).
30. J. Polchinski and M. J. Strassler, “The string dual of a confining four-dimensional gauge theory”, [hep-th/0003136](#).
31. I. R. Klebanov and M. J. Strassler, “Supergravity and a confining gauge theory: Duality cascades and χ SB-resolution of naked singularities”, *JHEP* **08** (2000) 052, [hep-th/0007191](#).
32. J. M. Maldacena and C. Nuñez, “Towards the large N limit of pure $N = 1$ super Yang Mills”, *Phys. Rev. Lett.* **86** (2001) 588–591, [hep-th/0008001](#).
33. O. Aharony, “The non-AdS/non-CFT correspondence, or three different paths to QCD”, [hep-th/0212193](#).
34. A. Karch and E. Katz, “Adding flavor to AdS/CFT”, *JHEP* **06** (2002) 043, [hep-th/0205236](#).
35. T. Sakai and J. Sonnenschein, “Probing flavored mesons of confining gauge theories by supergravity”, *JHEP* **09** (2003) 047, [hep-th/0305049](#).
36. T. Sakai and S. Sugimoto, “Low energy hadron physics in holographic QCD”, *Prog. Theor. Phys.* **113** (2005) 843–882, [hep-th/0412141](#).
37. J. Babington, J. Erdmenger, N. J. Evans, Z. Guralnik, and I. Kirsch, “Chiral symmetry breaking and pions in non-supersymmetric gauge/gravity duals”, *Phys. Rev.* **D69** (2004) 066007, [hep-th/0306018](#).
38. M. Kruczenski, D. Mateos, R. C. Myers, and D. J. Winters, “Towards a holographic dual of large- N_c QCD”, *JHEP* **05** (2004) 041, [hep-th/0311270](#).
39. R. Casero, E. Kiritsis, and A. Paredes, “Chiral symmetry breaking as open string tachyon condensation”, *Nucl. Phys.* **B787** (2007) 98–134, [hep-th/0702155](#).
40. M. Kruczenski, L. A. P. Zayas, J. Sonnenschein, and D. Vaman, “Regge trajectories for mesons in the holographic dual of large- N_c QCD”, *JHEP* **06** (2005) 046, [hep-th/0410035](#).
41. T. Sjöstrand, “The Lund Monte Carlo for jet fragmentation”, *Comp. Phys. Commun.* **27** (1982) 243.
42. B. Andersson, G. Gustafson, G. Ingelman, and T. Sjöstrand, “Parton fragmentation and string dynamics”, *Phys. Rep.* **97** (1983) 31.
43. A. Casher, H. Neuberger, and S. Nussinov, “Chromoelectric flux tube model of particle production”, *Phys. Rev.* **D20** (1979) 179–188.
44. K. S. Gupta and C. Rosenzweig, “Semiclassical decay of excited string states on leading regge trajectories”, *Phys. Rev.* **D50** (1994) 3368–3376, [hep-ph/9402263](#).
45. K. Peeters, J. Sonnenschein, and M. Zamaklar, “Holographic decays of large-spin mesons”, *JHEP* **02** (2006) 009, [hep-th/0511044](#).
46. O. Aharony, J. Sonnenschein, and S. Yankielowicz, “A holographic model of deconfinement and chiral symmetry restoration”, *Ann. Phys.* **322** (2007) 1420–1443, [hep-th/0604161](#).
47. K. Peeters, J. Sonnenschein, and M. Zamaklar, “Holographic melting and related properties of mesons in a quark gluon plasma”, *Phys. Rev.* **D74** (2006) 106008, [hep-th/0606195](#).
48. F. Karsch, “Lattice QCD at finite temperature and density”, *Nucl. Phys. Proc. Suppl.* **83** (2000) 14–23, [hep-lat/9909006](#).
49. S. A. Gottlieb *et al.*, “Thermodynamics of lattice QCD with two light quark flavours on a $16^3 \times 8$ lattice. II”, *Phys. Rev.* **D55** (1997) 6852–6860, [hep-lat/9612020](#).
50. E. V. Shuryak, “What RHIC experiments and theory tell us about properties of quark-gluon plasma?”, *Nucl. Phys.* **A750** (2005) 64–83, [hep-ph/0405066](#).
51. D. Teaney, “Effect of shear viscosity on spectra, elliptic flow, and Hanbury Brown-Twiss radii”, *Phys. Rev.* **C68** (2003) 034913, [nucl-th/0301099](#).
52. D. T. Son and A. O. Starinets, “Viscosity, black holes, and quantum field theory”, [arXiv:0704.0240 \[hep-th\]](#).

53. C. P. Herzog, A. Karch, P. Kovtun, C. Kozcaz, and L. G. Yaffe, “Energy loss of a heavy quark moving through $N=4$ supersymmetric Yang-Mills plasma”, *JHEP* **07** (2006) 013, [hep-th/0605158](#).
54. S. S. Gubser, “Drag force in AdS/CFT”, *Phys. Rev.* **D74** (2006) 126005, [hep-th/0605182](#).
55. P. Burikham and J. Li, “Aspects of the screening length and drag force in two alternative gravity duals of the quark-gluon plasma”, *JHEP* **03** (2007) 067, [hep-ph/0701259](#).
56. A. Buchel, “On jet quenching parameters in strongly coupled non- conformal gauge theories”, *Phys. Rev.* **D74** (2006) 046006, [hep-th/0605178](#).
57. N. Armesto, J. D. Edelstein, and J. Mas, “Jet quenching at finite ’t Hooft coupling and chemical potential from AdS/CFT”, *JHEP* **09** (2006) 039, [hep-ph/0606245](#).
58. O. Kaczmarek and F. Zantow, “Static quark anti-quark interactions in zero and finite temperature QCD. I: Heavy quark free energies, running coupling and quarkonium binding”, *Phys. Rev.* **D71** (2005) 114510, [hep-lat/0503017](#).
59. H. Liu, K. Rajagopal, and U. A. Wiedemann, “An AdS/CFT calculation of screening in a hot wind”, *Phys. Rev. Lett.* **98** (2007) 182301, [hep-ph/0607062](#).
60. M. Chernicoff, J. A. Garcia, and A. Guijosa, “The energy of a moving quark-antiquark pair in an $N=4$ SYM plasma”, *JHEP* **09** (2006) 068, [hep-th/0607089](#).